Ohmic contacts on n-type β-Ga_2O_3 using AZO/Ti/Au

Patrick H. Carey, Jiancheng Yang, F. Ren, David C. Hays, S. J. Pearton, Soohwan Jang, Akito Kuramata, and Ivan I. Kravchenko

Citation: AIP Advances **7**, 095313 (2017); doi: 10.1063/1.4996172
View online: https://doi.org/10.1063/1.4996172
View Table of Contents: http://aip.scitation.org/toc/adv/7/9
Published by the American Institute of Physics

AIP ADVANCES **7**, 095313 (2017)

Ohmic contacts on n-type β-Ga_2O_3 using AZO/Ti/Au

Patrick H. Carey IV,[1] Jiancheng Yang,[1] F. Ren,[1] David C. Hays,[2]
S. J. Pearton,[2,a] Soohwan Jang,[3] Akito Kuramata,[4] and Ivan I. Kravchenko[5]
[1]*Department of Chemical Engineering, University of Florida, Gainesville, FL 32611, USA*
[2]*Department of Materials Science and Engineering, University of Florida, Gainesville, FL 32611, USA*
[3]*Department of Chemical Engineering, Dankook University, Yongin 16890, Korea*
[4]*Tamura Corporation, Sayama, Saitama 350-1328, Japan and Novel Crystal Technology, Inc., Sayama, Saitama 350-1328, Japan*
[5]*Center for Nanophase Materials Sciences, Oak Ridge National Laboratory, Oak Ridge, Tennessee 37830, USA*

(Received 14 July 2017; accepted 24 August 2017; published online 14 September 2017)

AZO interlayers between n-Ga_2O_3 and Ti/Au metallization significantly enhance Ohmic contact formation after annealing at ≥ 300°C. Without the presence of the AZO, similar anneals produce only rectifying current-voltage characteristics. Transmission Line Measurements of the Au/Ti/AZO/Ga_2O_3 stacks showed the specific contact resistance and transfer resistance decreased sharply from as-deposited values with annealing. The minimum contact resistance and specific contact resistance of 0.42 Ω-mm and 2.82×10^{-5} Ω-cm^2 were achieved after a relatively low temperature 400°C annealing. The conduction band offset between AZO and Ga_2O_3 is 0.79 eV and provides a favorable pathway for improved electron transport across this interface. [http://dx.doi.org/10.1063/1.4996172]

There is significant promise in β-Ga_2O_3 for use in electronics for extreme environments (high temperature, high radiation and high voltage switching)[1–15] and for solar blind UV detection.[16] Ga_2O_3 is suited to these applications because of its wide bandgap, ~4.8 eV and high theoretical critical field strength ~8 MV/cm (experimental values have reached 3.8 MV/cm).[13] Ga_2O_3 bulk and epitaxial crystals can be grown by many methods including Czochralski, edge-defined film-fed growth (EFG), Verneuil, float-zone, molecular beam epitaxy (MBE), halide vapor phase epitaxy growth (HVPE), with excellent control of quality and n-type conductivity.[1,2,14,15,17] The β-phase of Ga_2O_3 has a monoclinic structure and is the most commonly studied of the different polymorphs.[1,2,18–21] Excellent results for β-Ga_2O_3-based power rectifiers, field effect transistors (FETs) and metal-oxide FETs (MOSFETs) have been reported,[2,4–13] along with solar blind photodetectors.[1,2,16] In all cases, these devices would benefit from an improved low resistance Ohmic contacting process that requires only moderate annealing temperatures.[4,8]

To date, the lowest specific contact resistance of ~4.6×10^{-6} Ω-cm^2 was reported for Ti/Au contacts on n-Ga_2O_3 epitaxial layers with Si implanted and annealed at 925°C followed by dry etching, metal deposition and annealing at 470°C.[21] Yao et al. explored nine different metals with Au capping layers to form Ohmic contact on Ga_2O_3, with many current-voltage (I-V) results being pseudo-Ohmic, and the best results obtained using Ti/Au.[22] For a metal deposited on an n-type semiconductor to achieve Ohmic contact requires the work function of the metal to be close or smaller than the electron affinity of the semiconductor. The reported electron affinity of β-Ga_2O_3 is ~4.00 ± 0.05 eV,[23,24] which limits the available options of metals.

Another option is to use a transparent conducting oxide (TCO) as an interlayer between the metal and substrate. Traditionally, the most used TCO is indium tin oxide (ITO), which combines

---

[a] Corresponding author: spear@mse.ufl.edu

high conductivity and optical transparency in the visible region of the spectrum. Previous reports of sputtered ITO as an intermediary layer for forming Ohmic contacts on Ga_2O_3 also needed high temperature annealing to produce good quality contacts.[25] A Pt/ITO bi-layer contact to β-Ga_2O_3 showed superior Ohmic contact properties compared to Pt/Ti and this was ascribed to the formation of an interfacial layer with lower bandgap and higher doping concentration than the Ga_2O_3.[25] The band alignment at the heterointerface is critically important in determining the favorability of carrier transport. AZO is another alternative that is widely used as a TCO with lower cost relative to ITO.[26] AZO has been heavily studied for transparent and flexible device applications such as display panels, gas sensors, organic light emitting diodes, and other optoelectronic devices.[27–32]

In this letter, we report on the use of AZO interlayers in facilitating Ohmic behavior in Ti/Au contacts on n-type, Si implanted β-Ga_2O_3. The minimum specific contact resistance of 2.82×10^{-5} Ω-cm^2 was achieved after annealing at 400°C. By sharp contrast, Ti/Au contacts without the AZO did not lead to Ohmic behavior.

The samples used were bulk 2in. β-Ga_2O_3 single crystal wafers with (-201) surface orientation grown by EFG. Hall measurements showed these were n-type (electron concentration of $\sim 2.2\times10^{17}$ cm^{-3}). Si^+ implantation was performed at an energy of 30 keV with a dose of 1×10^{15} cm^{-2} into the front surface of the samples, which were then annealed at 950°C to activate the implanted ions and increase the surface conductivity.

We deposited 10 nm of AZO by RF magnetron sputtering on the Si implanted β-Ga_2O_3 at ~30°C using a 3-in. diameter composite AZO (Al_2O_3/ZnO_2 2/98 wt %) target. The RF power was 125 W and the pressure was 5×10^{-6} Torr in a pure Ar ambient. The DC bias on the electrode was in the range of 30-40V. The contact metal pads (100 μm on a side) for transmission line method (TLM) testers were formed by standard lift-off of E-beam deposited Ti/Au (20 nm/80 nm) metallization. AZO was wet etched from between the contact pads using 1:10 HCl:DI water. Cl_2/Ar dry etching was used to define the 0.5 μm deep mesas of TLM test patterns prior to AZO deposition in a Plasma-Therm Versaline inductively coupled plasma (ICP) tool at 300 W (2 MHz) ICP power and 150 rf (13.56 MHz) chuck power (dc self-bias of -150V on the sample electrode). A SSI Solaris 150 rapid thermal annealing system was used to anneal the contact in the nitrogen ambient. Figure 1 shows a schematic of the contact stack structures with and without AZO interlayers. The contact properties were measured over the range 25-150°C. Current-voltage (I-V) characteristics were measured with an Agilent 4145B parameter analyzer.

We previously determined the valence and conduction band offsets in rf-sputtered AZO and single crystal β-Ga_2O_3 heterostructures.[33] The bandgaps of the component materials were 4.6 eV for Ga_2O_3 and 3.2 eV for AZO, with AZO/Ga_2O_3 system having a nested gap (type I) alignment, as shown in Figure 2. Thus, use of a thin layer of AZO has the ability to reduce the barrier for electron transport and hence the contact resistance between the metal and Ga_2O_3.

The I-V characteristics of Ti (20nm)/Au(80nm) on β-Ga_2O_3, annealed at temperatures of 300, 400, 500, and 600°C, all demonstrated high resistance Schottky behavior (Figure 3a). Introduction of the AZO interlayer significantly improved current transport (Figure 3b). Low temperature annealing further improved the Ohmic behavior, with compliance of 100 mA reached first by the sample annealed at 400°C. Increasing annealing temperature further did not improve performance. In previous works, annealing above 300°C has been found to decrease the carrier concentration and electron mobility within the AZO layer[26–30] thus a lower current flow would be expected from higher annealing

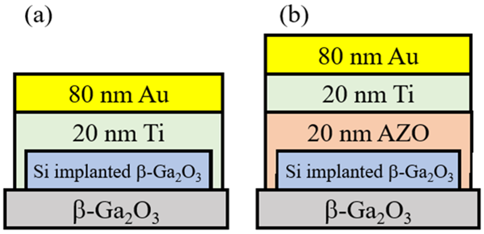

FIG. 1. Schematic of (a) Au/Ti and (b) Au/Ti/AZO contact stack on Si-implanted Ga_2O_3.

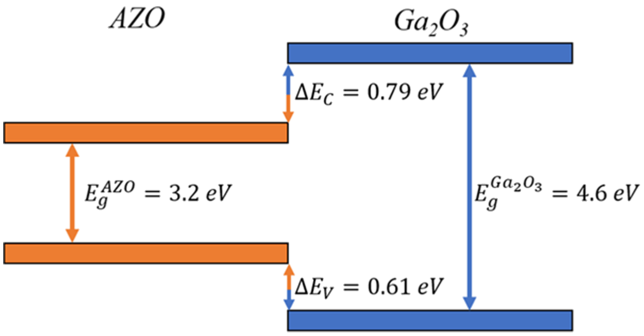

FIG. 2. Schematic of band offset for AZO on Ga_2O_3.

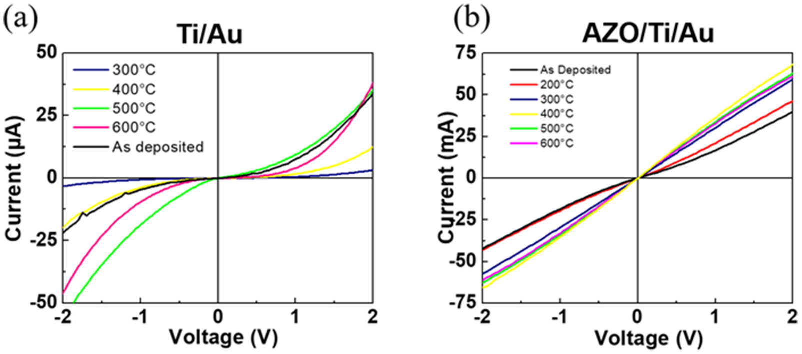

FIG. 3. I-V of (a) Au/Ti/Ga_2O_3 and (b) Au/Ti/AZO/Ga_2O_3 contact stacks as a function of annealing temperatures from as-deposited (black lines) to 600°C (purple lines). The 200°C data is similar to the as-deposited and the contact resistance decreases with temperature in the AZO-based contacts.

temperatures and can be seen when comparing the I-V curves of annealing temperatures 400°C and 600°C.

The TLM data was used to extract the sheet resistance (R_S), specific contact resistance (R_C), and transfer resistance (R_T). A sample output resistance vs. gap size from AZO contact stack annealed at 400°C is shown in Figure 4, and a strong linear dependence ($r^2 = 0.991$) is observed. The sheet resistance had a minimum of 41 Ω/ after 200°C annealing (Figure 5) due to incomplete removal of sputter induced damage. Transfer and specific contact resistance had minimums of 0.42 Ω-mm and 2.82 x 10^{-5} Ω-cm^2, respectively, both after annealing at 400°C (Figure 5). Initially, all resistances decrease due to interaction between the AZO and Ga_2O_3 and removal of damage from the ion bombardment from sputtering, but as the crystallinity of the AZO layer improves above 400°C, the

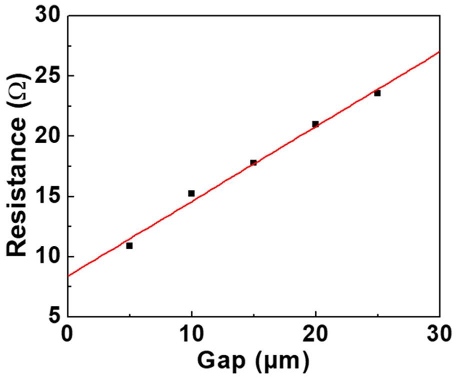

FIG. 4. TLM data of Au/Ti/AZO/Ga_2O_3 contact stack resistance as a function of gap spacing.

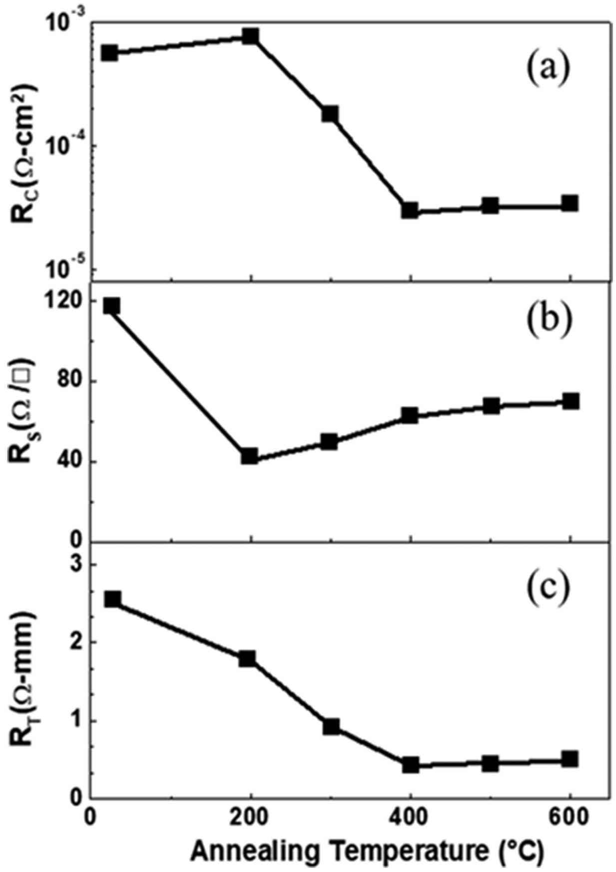

FIG. 5. Sheet resistance, specific contact resistance and transfer resistance as a function of annealing temperature for Au/Ti/AZO/Ga_2O_3 contact stack.

flow through the layer is inhibited slightly. It will be important to perform future studies of the contacts with transmission electron microscopy to understand any changes in interfacial structure and the role of both AZO thickness and choice of metal. We did find that annealing of the bare Ga_2O_3 up to 600°C did not affect the carrier density or mobility of the layers.

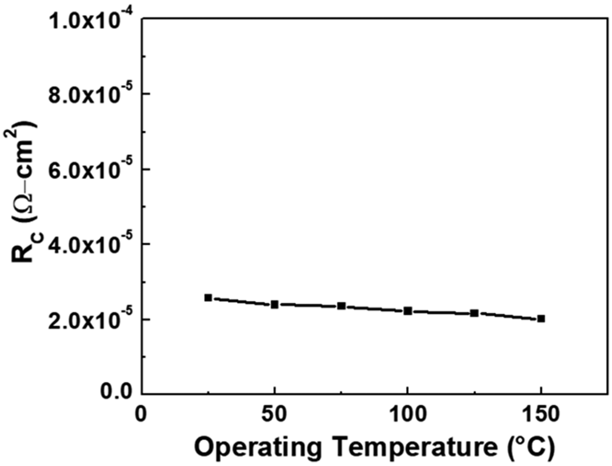

FIG. 6. Specific contact resistance, R_c, as a function of measurement temperature for a Au/Ti/AZO/Ga_2O_3 contact stack initially annealed at 400°C for 30 secs.

The effect of operating temperature was also explored on a Ti/Au/AZO/Ga_2O_3 stack annealed at 400°C in N_2 for 30 seconds. The temperature was increased from 25°C to 150°C in increments of 25°C. As the temperature rose, minimal change in specific contact resistance was observed (Figure 6), this is an advantage for high temperature power device application. With these operating temperatures, no degradation of the contact was observed.

In summary, the inclusion of AZO interlayers on Ti/Au contacts to n-type Ga_2O_3 was found to enhance electron transport across the heterointerface, leading to Ohmic behavior. The band alignment of AZO on Ga_2O_3 reduces the barrier for conduction. Au/Ti/AZO/Ga_2O_3 contact stacks exhibit minimum contact resistance and specific contact resistance of 0.42 Ω-mm and 2.82 x 10^{-5} Ω-cm^2, respectively, after annealing at a relatively low temperature of 400°C. Without the AZO, similar anneals did not lead to linear current-voltage characteristics of Au/Ti/Ga_2O_3 contact layers. Future studies should focus on an examination of the transport mechanism in the AZO-based contacts and changes in the interfacial structure with annealing.

ACKNOWLEDGMENTS

The project or effort depicted was also sponsored by the Department of the Defense, Defense Threat Reduction Agency, HDTRA1-17-1-011, monitored by Jacob Calkins. A portion of this research was conducted at the Center for Nanophase Materials Sciences, which is sponsored at Oak Ridge National Laboratory by the Office of Basic Energy Sciences, U.S. Department of Energy. The content of the information does not necessarily reflect the position or the policy of the federal government, and no official endorsement should be inferred. The research at Dankook was supported by the Basic Science Research Program through the National Research Foundation of Korea (NRF) funded by the Ministry of Education (2015R1D1A1A01058663), and Nano Material Technology Development Program through the National Research Foundation of Korea (NRF) funded by the Ministry of Science, ICT and Future Planning (2015M3A7B7045185). Part of the work at Tamura was supported by "The research and development project for innovation technique of energy conservation" of the New Energy and Industrial Technology Development Organization (NEDO), Japan. We also thank Dr. Kohei Sasaki from Tamura Corporation for fruitful discussions. A portion of this research was conducted at the Center for Nanophase Materials Sciences, which is a DOE Office of Science User Facility.

[1] H. von Wenckstern, Adv. Electron. Mat.1600350 (2017).
[2] M. A. Mastro, A. Kuramata, J. Calkins, J. Kim, F. Ren, and S. J. Pearton, ECS J. Solid State Sci. Technol. **6**, P356 (2017).
[3] M. Tadjer, N. A. Mahadik, V. D. Wheeler, E. R. Glaser, L. Ruppalt, A. D. Koehler, K. D. Hobart, C. R. Eddy, Jr., and F. J. Kub, ECS J. Solid State Sci.Technol. **5**, P468 (2016).
[4] K. D. Chabak, N. Moser, A. J. Green, D. E. Walker, Jr., S. E. Tetlak, E. Heller, A. Crespo, R. Fitch, J. P. McCandless, K. Leedy, M. Baldini, G. Wagner, Z. Galazka, and G. Jessen, Appl. Phys. Lett. **109**, 213501 (2016).
[5] K. Sasaki, A. Kuramata, T. Masui, and S. Yamakoshi, IEEE Electron Dev. Lett **34**, 493 (2013).
[6] Z. Galazka, K. Irmscher, R. Uecker, R. Bertram, M. Pietsch, A. Kwasniewski, M. Naumann, T. Schulz, R. Schewski, D. Klimm, and M. Bickermann, J. Cryst. Growth **404**, 184 (2014).
[7] W. S. Hwang, A. Verma, H. Peelaers, V. Protasenko, S. Rouvimov, H. Xing, A. Seabaugh, W. Haensch, C. Van de Walle, Z. Galazka, M. Albrecht, R. Fornari, and D. Jena, Appl. Phys. Lett. **104**, 203111 (2014).
[8] M. Higashiwaki, K. Sasaki, H. Murakami, Y. Kumagai, A. Koukitu, A. Kuramata, T. Masui, and S. Yamakosh, Semicond. Sci. Technol. **31**, 034001 (2016).
[9] N. A. Moser, J. P. McCandless, A. Crespo, K. D. Leedy, A. J. Green, E. R. Heller, K. D. Chabak, N. Peixoto, and G. H. Jessen, Appl. Phys. Lett. **110**, 143505 (2017).
[10] M. H. Wong, K. Sasaki, A. Kuramata, S. Yamakoshi, and M. Higashiwaki, IEEE Electron Dev. Lett. **37**, 212 (2016).
[11] S. Ahn, F. Ren, J. Kim, S. Oh, J. Kim, M. A. Mastro, and S. J. Pearton, Appl. Phys. Lett. **109**, 062102 (2016).
[12] J. Kim, S. Oh, M. Mastro, and J. Kim, Phys. Chem. Chem Phys. **18**, 15760 (2016).
[13] A. J. Green, K. D. Chabak, E. R. Heller, R. C. Fitch, Jr., M. Baldini, A. Fiedler, K. Irmscher, G. Wagner, Z. Galazka, S. E. Tetlak, A. Crespo, K. Leedy, and G. H. Jessen, IEEE Electron Dev. Lett. **37**, 902 (2016).
[14] S. Rafique, L. Han, A. T. Neal, S. Mou, M. J. Tadjer, R. H. French, and H. Zhaoless, Appl. Phys. Lett. **109**, 132103 (2016).
[15] H. Murakami, K. Nomura, K. Goto, K. Sasaki, K. Kawara, Q. T. Thieu, R. Togashi, Y. Kumagai, M. Higashiwaki, A. Kuramata, S. Yamakoshi, B. Monemar, and A. Koukitu, Appl. Phys. Express **8**, 015503 (2015).
[16] Z. Zhang, H. von Wenckstern, J. Lenzner, M. Lorenz, and M. Grundmann, Appl. Phys. Lett. **108**, 123503 (2016).
[17] K. Irmscher, Z. Galazka, M. Pietsch, R. Uecker, and R. Fornari, J. Appl. Phys. **110**, 063720 (2011).
[18] M. Steffens, R. Vianden, and A. F. Pasquevich, Hyperfine Interact **237**, 117 (2016).
[19] L. M. Foster and H. C. Stumpf, J. Am. Chem. Soc. **73**, 1590 (1951).
[20] S. C. Abrahams, J. M. Reddy, and J. L. Bernstein, J. Chem. Phys. **42**, 3957 (1965).

[21] K. Sasaki, M. Higashiwaki, A. Kuramata, T. Masui, and S. Yamakoshi, Appl. Phys. Express **6**, 086502 (2013).

[22] Y. Yao, R. F. Davis, and L. M. Porter, J. Electron Mater. **46**, 2053 (2016).

[23] V. D. Wheeler, D. I. Shahin, M. J. Tadjer, and C. R. Eddy, Jr., ECS J. Solid State Sci. Technol. **6**, Q3052 (2017).

[24] M. Mohamed, K. Irmscher, C. Janowitz, Z. Galazka, R. Manzke, and R. Fornari, Appl. Phys. Lett. **101**, 132106 (2012).

[25] T. Oshima, R. Wakabayashi, M. Hattori, A. Hashiguchi, N. Kawano, K. Sasaki, T. Masui, A. Kuramata, S. Yamakoshi, K. Yoshimatsu, A. Ohtomo, T. Oishi, and M. Kasu, Jpn. J. Appl. Phys. **55**, 1202B7 (2016).

[26] T. M. Miyata, Thin Solid Films **517**, 1474 (2008).

[27] L. Dejam, M. Elahi, H. H. Nazari, H. Elahi, S. Solaymani, and A. Ghaderi, J Mater Sci: Mater Electron **27**, 685 (2016).

[28] T.-Y. Yun, S.-R. Park, J.-Y. Baek, H.-J. Han, and C.-W. Jeon, Mol. Cryst. Liquid Cryst. **586**, 82 (2013).

[29] R. Pandey, S. Yuldashev, H. D. Nguyen, H. C. Jeon, and T. W. Kang, Current Appl. Phys. **12**, s56 (2012).

[30] A. Varanytsia, L. Weng, T.-C. Lin, J. Yang, and L.-C. Chien, J. Display Technol. **12**, 1033 (2016).

[31] J. Loureiro, N. Neves, R. Barros, T. Mateus, R. Santos, S. Filonovich, S. Reparaz, C. M. Sotomayor-Torres, F. Wyczisk, L. Divay, R. Martins, and I. Ferreira, J. Mater. Chem. A **2**, 6649 (2014).

[32] D. Ginley, H. Hosono, and D. C. Paine, *Handbook of Transparent Conductors* (Springer, 2011).

[33] P. H. Carey IV, F. Ren, D. C. Hays, B. P. Gila, S. J. Pearton, S. Jang, and A. Kuramata, Vacuum **141**, 103 (2017).